Intensities in the $^3\Pi$, $^3\Sigma$ Band of PH

PHILIP NOLAN* AND F. A. JENKINS, *Department of Physics, University of California, Berkeley, California*

(Received September 3, 1936)

Measurements of the relative intensities of the lines in the 0,0 band of PH at λ3400 are given. The band was excited by a high voltage discharge through hydrogen and phosphorus vapor. The distribution of molecules in the initial states is evaluated by using the sum rule, and is found to correspond to thermal equilibrium at 696°K, not only for the various rotational levels of a given electronic state, but also for the three components of the $^3\Pi$ multiplet. The intensity factors i are tabulated and compared with their theoretical values for $^3\Pi$ (case a), $^3\Sigma$ and for $^3\Pi$ (case b), $^3\Sigma$. These theoretical factors are given for the first time in explicit form. The observed i factors are in qualitative agreement with theory. For the main branches, they are linear functions of J', with relative values close to those expected for case b at all except the lowest J values. For the satellite branches, they increase nearly linearly at low J, but soon reach a maximum and fall off, due to the uncoupling of the spin by the rotation. From the experimental i factors, the sum rule is also verified for the lower states.

VERY few experimental data on the intensities of the rotational structure in multiplet bands have thus far appeared, in spite of the existence of a fairly complete theory of the intensity distribution in such bands. Of the band systems showing an appreciable electronic multiplet separation, only the $^3\Pi$, $^3\Pi$ bands[1] of N_2 and the $^2\Pi$, $^2\Sigma$ bands[2] of HgH have been investigated quantitatively. The $^3\Pi$, $^3\Sigma$ system of PH analyzed by Pearse[3] presents a favorable case for accurate intensity measurements, since the 0,0 band at λ3400, which is the only one of any intensity, has an open structure free from overlapping by other bands. Pearse showed that the $^3\Pi$ state is inverted, with separations $^3\Pi_0-{}^3\Pi_1=121$ cm^{-1} and $^3\Pi_1-{}^3\Pi_2=111$ cm^{-1}. All of the 27 branches predicted for a coupling in the $^3\Pi$ state intermediate between case a and case b were identified. Theoretical intensity factors have not been derived for the intermediate case, although they are available for the two limiting cases $^3\Pi$ (case a), $^3\Sigma$ and $^3\Pi$ (case b), $^3\Sigma$, between which the actual case lies. For this reason, only a qualitative comparison of the experimental i factors with theory can be made, but it will be shown that the principal features of these are well accounted for. In addition, application of the intensity sum rules has made possible the determination of the distribution of molecules in the initial states under the conditions of excitation used.

* Now at the Institute of Paper Chemistry, Appleton Wisconsin.

[1] W. R. van Wijk, Zeits. f. Physik **59**, 313 (1930).

[2] W. Kapuscinski and J. G. Eymers, Zeits. f. Physik **54**, 246 (1929); J. G. Eymers, Zeits. f. Physik **63**, 396 (1930).

[3] R. W. B. Pearse, Proc. Roy. Soc. **A129**, 328 (1930).

EXPERIMENTAL PROCEDURE

The discharge tube was similar to that described by Pearse.[3] Phosphorus is continuously vaporized into a stream of hydrogen flowing through the capillary of an ordinary end-on tube. The hydrogen pressure was 1.5 to 2.0 mm on the high pressure side of the 2 mm capillary, and a discharge current of 45 m amp. was maintained by a 25 kv transformer. The spectrum was photographed in the first three orders of the 21-foot concave grating, which has a dispersion of 1.29A/mm at λ3400 in the second order. It was necessary to use a slit as narrow as 0.025 mm, in order to suppress as far as possible the continuous spectrum of hydrogen, which always accompanied the PH spectrum. Plates were developed $4\frac{1}{2}$ minutes in 1 : 20 Rodinal at 18°C, and the standard precautions for uniform development were taken.

Each plate carried a set of intensity calibrations, produced by a platinum-on-quartz step-weakener having seven steps 1.5 mm wide and 27 mm long. The step-weakener was placed 1.5 cm in front of the plate, normal to the incident light, so that each spectrum line produced calibration marks of the same width and character as the lines of the direct spectrum. The transmissions of the steps for the wave-length used were measured by a photographic method, in which the blackenings produced by the continuous H_2 spectrum photographed through the step-weakener in the above position were compared with those produced on the same plate by three different neutral methods of intensity reduction: neutral screens, the step-slit (used in

TABLE I. *Intensities and i factors in the 0,0 band of PH at λ3400.*

	P_1		Q_1		R_1		P_2		Q_2		R_2		P_3		Q_3		R_3	
J'	I	i	I	i	I	i	I	i	I	i	I	i	I	i	I	i	I	i
0													8	18	8	22		
1									28	$R_{23}(2)$			15	43	19	54	12	$P_{31}(1)$
2	18	33	58	$Q_{23}(5)$	105	$Q_1(4)$	5	12	11	26	79	$R_2(2)$	23	69	31	92	15	$P_{31}(2)$
3	35	$R_{13}(4)$	130	270	78	153	11	31	21	56	66	$R_1(9)$	36	121	51	171	26	$P_{31}(3)$
4	59	$P_3(8)$ $P_1(4)$	105	$R_1(1)$	79	173			36	110	16	49	85	$Q_2(10)$ $Q_{23}(2)$	63	243	26	100
5	46	117	133	342	92	232	86	$R_{12}(2)$	47	168	22	79	53	255	75	350	60	$R_{21}(5)$
6	56	173	140	412	86	266	28	123	61	265	64	$R_1(12)$	42	250	76	445	33	190
7	61	232	144	520	88	329	29	165	65	358	31	166	39	298	71	530	33	244
8	59	280	144	660	79	$R_2(2)$	30	216	65	$P_2(11)$	30	210	52	$R_{13}(4)$	63	630	28	280
9	50	320	123	745	67	$R_2(3)$	26	248	59	554	30	275	42	$P_{23}(4)$	54	745	24	330
10	49	420	96	790	53	440	22	300	85	$Q_{23}(2)$	22	285			42	840	19	381
11	32	400	74	890	43	514	20	$R_{13}(10)$	36	670	41	$Q_{32}(1)$	35	$P_{12}(4)$	28	800	14	400
12	24	440			67	$R_2(6)$	12	340	72	$Q_{23}(3)$			21	$R_{12}(5)$			24	$R_{21}(6)$
13	21	550	41	1120	23	620	9	400	12	$P_{23}(1)$								
14			26	1130	14	600												
15			18	1200	34	$Q_{21}(8)$												
16			12	1280														

	${}^{Q}P_{21}$		${}^{R}Q_{21}$		${}^{S}R_{21}$		${}^{Q}P_{32}$		${}^{R}Q_{32}$		${}^{S}R_{32}$		${}^{R}P_{13}$		${}^{S}Q_{31}$		${}^{T}R_{13}$	
J'	I	i	I	i	I	i	I	i	I	i	I	i	I	i	I	i	I	i
0							18	50										
1			31	67			28	79	42	$R_2(11)$					13	$P_{31}(5)$		
2	41	97	50	117	22	52	31	92	40	120	10	30			17	$Q_{32}(10)$		
3	70	$R_{23}(3)$	61	157	28	73	33	111	45	151	12	40			10	30		
4	55	$R_{23}(4)$	64	188	27	80	32	126	48	184	13	50	12	46	8	30	2	
5	35	125	55	192	58	$R_3(5)$	29	134	41	191	12	56			5	22		
6	28	122	52	221	24	$R_3(12)$	21	123	33	192	11	60			9	$R_{21}(9)$		
7	92	$R_1(5)$	41	222	17	93	21	157	25	184	9	66			3	22		
8	40	$Q_{23}(1)$	34	$R_1(15)$	13	76	16	$R_{23}(1)$	19	188	5	50						
9	11	106	23	$R_1(18)$	9	86	11	156	14	191								
10	9	123	13	169	6	82			11	$Q_{31}(2)$								
11	5	99	15	269	3	57			6	170								
12									12	?								

	${}^{O}P_{12}$		${}^{P}Q_{12}$		${}^{Q}R_{12}$		${}^{O}P_{23}$		${}^{P}Q_{23}$		${}^{Q}R_{23}$		${}^{N}P_{13}$		${}^{O}Q_{13}$		${}^{P}R_{13}$	
J'	I	i	I	i	I	i	I	i	I	i	I	i	I	i	I	i	I	i
0																		
1							14	32										
2	9	16	40	72	91	$P_2(5)$	17	41			29	$Q_2(1)$			11	19	9	16
3	61	$Q_{12}(9)$	66	128	82	160	22	59	73	$Q_{12}(12)$	70	$P_{21}(3)$				$R_{13}(9)$	35	$P_1(4)$
4	33	$P_3(10)$	79	174	74	162	46	$P_3(8)$			55	$P_{21}(4)$			10	23	59	$P_1(5)$
5	20	$P_3(11)$	79	203	81	210	17	62	57	$Q_1(2)$	40	143			9	24	16	$P_3(8)$ 41
6			74	228	61	190	15	66	47	208	33	141			8	24		
7	19	73	63	240	47	$R_{12}(8)$			37	208	34	186			5	19	19	73
8			56	$P_{12}(3)$	47	$R_{12}(7)$	11	$P_{13}(4)$	27	190	21	149					14	67
9			33	210	96	$Q_{23}(4)$			21	204	13	123						
10			23	198	43				13	176	23	?						
11			14	175	16	180					6	122						
12			11	190					6	160								
13									4	180								

a prism spectrograph) and rotating sectors used centrally in a collimated beam.

The plates were photometered on the Zeiss recording microphotometer, and a separate calibration curve constructed for each plate. It was assumed that the plate characteristics, as well as the step-weakener transmissions, did not vary over the wave-length range of 80A covered by the band. The calibration curves drawn from several different lines were closely parallel, and the final curve was obtained by parallel displacement of these curves along the log I axis to obtain the best average coincidence. To obtain the intensity of a line, the intensity of the continuous background was subtracted from the peak intensity. In reducing the microphotometer curves, the mechanical ratiometer described by Langstroth[4] for drawing the density curves and reading intensities directly by settings on the projected image of the microphotometer trace was found convenient.

Table I gives the observed relative intensities I of all measurable lines, together with the resulting intensity factors i obtained in a manner explained below. The intensities given represent average values from three second-order plates and one third-order plate. In the case of known blends the intensity given is the total, measured value, and the designation of the blended line or lines appears in place of the i factor. The errors of measurement should not exceed about 3 percent for lines which are clearly resolved.

Interpretation of The Results

The intensity of any band line may be conveniently written[5]

$$I=k\nu^4 iR', \tag{1}$$

in which k may be considered as constant for the lines of any one band. The intensity factor i is a function of the rotational quantum number, and is independent of the excitation conditions, while R' is the number of molecules in the initial state divided by the statistical weight of that state. In most cases of electrical excitation, the function R' is experimentally found to have the form $e^{-E'r/kT}$ corresponding to the distribution among the rotational levels required for thermal equilibrium at the temperature T. The distribution between the vibrational levels, and between the components of wide electronic multiplet levels, on the other hand, has not been found to correspond even approximately to thermal equilibrium at this temperature.[2] Hence for the present we may write

$$I=g'\nu^4 ie^{-E_r/kT}, \tag{2}$$

leaving open the equation of the relative values of g' in the three sub-bands $^3\Pi_0\rightarrow{}^3\Sigma$, $^3\Pi_1\rightarrow{}^3\Sigma$ and $^3\Pi_2\rightarrow{}^3\Sigma$.

Distribution of molecules in the initial state

The existence of an effective temperature for rotation may be directly tested from the data, without any knowledge of the i factors, by applying the sum rules:

$$\sum_{J''} i=\text{const. } (2J'+1), \tag{3}$$

$$\sum_{J'} i=\text{const. } (2J''+1). \tag{4}$$

From Eq. (2):

$$\sum_{J''} I=g'\nu^4 e^{-E_r/kT}\sum_{J''} i, \tag{5}$$

neglecting the variation of ν^4 over the band. Hence by Eq. (3),

$$\sum_{J''} I=\text{const. } (2J'+1)e^{-E_r/kT}, \tag{6}$$

and $$\log\left(\sum_{J''} I/2J'+1\right)=-E_r/kT+\text{const.} \tag{7}$$

These summations have been carried out for the various initial states J' of the three sub-bands. Intensities of all blended lines of appreciable intensity were interpolated on graphs of the intensities of the various branches against J'. The results are given in Fig. 1a, where the ordinate is $F(J')$, the rotational term values in the upper states taken from Pearse's analysis, and the abscissa $\log R'=\log\left(\sum_{J''} I/2J'+1\right)$. Three lines are obtained for the three sub-bands $^3\Pi_0\rightarrow{}^3\Sigma$, $^3\Pi_1\rightarrow{}^3\Sigma$ and $^3\Pi_2\rightarrow{}^3\Sigma$, respectively, from left to right, the lines being straight and parallel within the experimental error. The temperatures derived by least squares from the slopes, $-1/kT$,

[4] G. O. Langstroth, Rev. Sci. Inst. **5**, 255 (1934).
[5] R. S. Mulliken, Rev. Mod. Phys. **3**, 100 (1931).

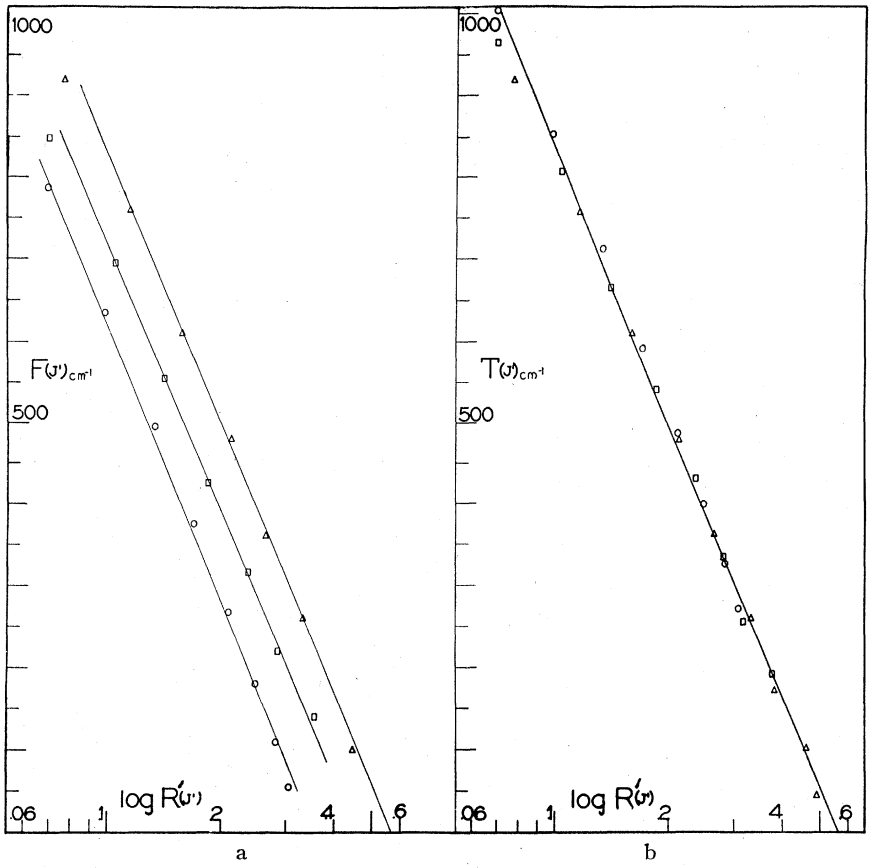

FIG. 1 (a). The rotational term values as a function of log R' where $R'=(\sum_{J''} I/2J'+1)$; (b) Total term value of upper state as a function of log R'.

of the three curves are 700°K, 694°K and 689°K, respectively.

It is seen that the band originating on the lowest level, $^3\Pi_2$, is relatively the strongest, as would be the case if thermal equilibrium determined the relative numbers of molecules in the multiplet components. Hence the results were replotted, as in Fig. 1b, against the total term value of the upper state $T(J')=F(J')+A\Lambda\Sigma$, where $A\Lambda\Sigma$ represents the electronic coupling energy. The fact that the three lines now become coincident shows not only the distribution of molecules between the electronic multiplet components corresponds to temperature equilibrium, but that the same temperature is effective for both electronic and rotational energy. This result is in marked contrast to that for HgH,[2] where, however, the multiplet separation is an order of magnitude greater. The difference shows definitely that with the small multiplet separation existing in PH, it is possible for the molecules to be redistributed by thermal impacts while in the excited state. In HgH, under the conditions used other processes evidently determined the relative numbers of molecules in the multiplet components. Besides the pressure, the ratio of the mean translational kinetic energy to the energy intervals involved play an important part.[6] The ratio of the spin coupling energy to kT is 5 to 1 for HgH, while it is only 1 to 5 for PH.

The intensity factors

No explicit i factors for $^3\Pi$, $^3\Sigma$ transitions could be found in the literature, although in principle they are contained in the general equations of Hill and Van Vleck.[7] The derivation of closed

[6] L. S. Ornstein and H. Brinkman, Physica **1**, 797 (1934).
[7] E. L. Hill and J. H. Van Vleck, Phys. Rev. **32**, 250 (1928).

TABLE II. *i factors for* $^3\Pi$, $^3\Sigma$ *transitions with ideal coupling.*

$^3\Pi$ (*case a*), $^3\Sigma$			$^3\Pi$ (*case b*), $^3\Sigma$		
$^3\Pi_2$, $^3\Sigma$					
$P_1: \frac{(J-1)J(J+2)}{(J+1)(2J+3)}$	$^OP_{12}: \frac{(J-1)J}{J+1}$	$^NP_{13}: \frac{(J-1)J}{2J+3}$	$P_1: \frac{(2J-3)(J-1)}{2J-1}$	$^OP_{12}: 0$	$^NP_{13}: 0$
$Q_1: \frac{(J-1)(J+2)}{J}$	$^PQ_{12}: \frac{(J-1)(J+2)(2J+1)}{J(J+1)}$	$^OQ_{13}: \frac{(J-1)(J+2)}{J+1}$	$Q_1: \frac{(J-3)(J-1)(2J+1)}{J^2}$	$^PQ_{12}: \frac{J-1}{J^2}$	$^OQ_{13}: 0$
$R_1: \frac{(J+1)(J+2)}{2J-1}$	$^QR_{12}: \frac{(J+1)(J+2)}{J}$	$^PR_{13}: \frac{(J-1)(J+1)(J+2)}{J(2J-1)}$	$R_1: \frac{J(2J+1)}{2J-1}$	$^QR_{12}: \frac{2J+1}{J^2}$	$^PR_{13}: \frac{J-1}{(2J-1)J^2(2J+1)}$
$^3\Pi_1$, $^3\Sigma$					
$^QP_{21}: \frac{2J(J+1)}{2J+3}$	$P_2: 0$	$^OP_{23}: \frac{2J(J+2)}{2J+3}$	$^QP_{21}: \frac{2J-1}{J^2}$	$P_2: \frac{(J+2)J^2}{(J+1)^2}$	$^OP_{23}: 0$
$^RQ_{21}: 2J$	$Q_2: 0$	$^PQ_{23}: 2(J+1)$	$^RQ_{21}: \frac{J+1}{J^2}$	$Q_2: \frac{(J^2+J-1)^2(2J+1)}{J^2(J+1)^2}$	$^PQ_{23}: \frac{J}{(J+1)^2}$
$^SR_{21}: \frac{2(J-1)(J+1)}{2J-1}$	$R_2: 0$	$^QR_{23}: \frac{2J(J+1)}{2J-1}$	$^SR_{21}: 0$	$R_2: \frac{(J^2-1)(J+1)}{J^2}$	$^QR_{23}: \frac{2J+3}{(J+1)^2}$
$^3\Pi_0$, $^3\Sigma$					
$^RP_{31}: \frac{(J+2)^2}{2J+3}$	$^QP_{32}: J+2$	$P_3: \frac{(J+1)(J+2)}{2J+3}$	$^RP_{31}: \frac{1}{4J(J+1)^2}$	$^QP_{32}: \frac{2J+1}{(J+1)^2}$	$P_3: \frac{(2J+1)(2J+7)}{2J+5}$
$^SQ_{31}: J+1$	$^RQ_{32}: 2J+1$	$Q_3: J$	$^SQ_{31}: 0$	$^RQ_{32}: \frac{J+2}{(J+1)^2}$	$Q_3: \frac{J(2J+1)(J+2)}{(J+1)^2}$
$^TR_{31}: \frac{(J-1)J}{2J-1}$	$^SR_{32}: J-1$	$R_3: \frac{(J-1)^2}{2J-1}$	$^TR_{31}: 0$	$^SR_{32}: 0$	$R_3: \frac{(2J-1)(J+2)}{2J+1}$

Note: J represents the J value of the upper state in all cases.

formulas to cover all intermediate types of coupling in the $^3\Pi$ state, as was done for $^2\Pi$, $^2\Sigma$, is probably not possible here, but they can be obtained for the limiting conditions $^3\Pi$ (case *b*), $^3\Sigma$ and $^3\Pi$ (case *a*), $^3\Sigma$. Table II gives these factors, which are here given explicitly for the first time. The case *a* factors were kindly communicated to us by Professor Van Vleck as the results of some unpublished work. They were derived by a modification of the intensity formulas for the intercombination bands $^1\Sigma$, $^3\Pi$ as given by Schlapp.[8] The case *b* factors were calculated for us by Dr. Melba Phillips in this laboratory, using a method suggested by Mulliken.[9] They are given by the relation

$$i(\text{case } b) = i(\text{case } a) \cdot i(\text{atomic}) \cdot N(\Delta K)$$

$$K \rightarrow J \qquad \Delta J,\ s \rightarrow s$$
$$\Lambda \rightarrow \Omega \qquad \Delta K,\ K \rightarrow l,$$

where the arrows represent the replacement of one quantum number by another. $N(\Delta K)$ is a normalizing factor such that

$$\sum_{\Delta J} i(\text{atomic}) \cdot N(\Delta K) = 1.$$

The band in question represents a stage of coupling intermediate between case *a* and case *b*, the spin coupling parameter A/B being -14.8. We expect a tendency toward case *a* for very small rotational quantum numbers, but with increasing rotation the i factors should approach those of case *b* rapidly. The i factors may be determined from the measured intensities, once the distribution function R' is known, since, from Eqs. (1)

$$i = \text{const.} \times (I/R') = \text{const.} \times I e^{T'/kT},$$

where T' is the value of the total initial term, electronic+rotational, and T the temperature, 696°K. These experimental i factors are given in Table I, following the observed intensities. In Fig. 2a they are compared, for the main branches ($\Delta J = \Delta K$) with the theoretical curves for case *a* (dotted lines) and case *b* (full lines). In this comparison, the slopes of the experimental and

[8] R. Schlapp, Phys. Rev. **39**, 806 (1932).
[9] R. S. Mulliken, Phys. Rev. **30**, 785 (1927).

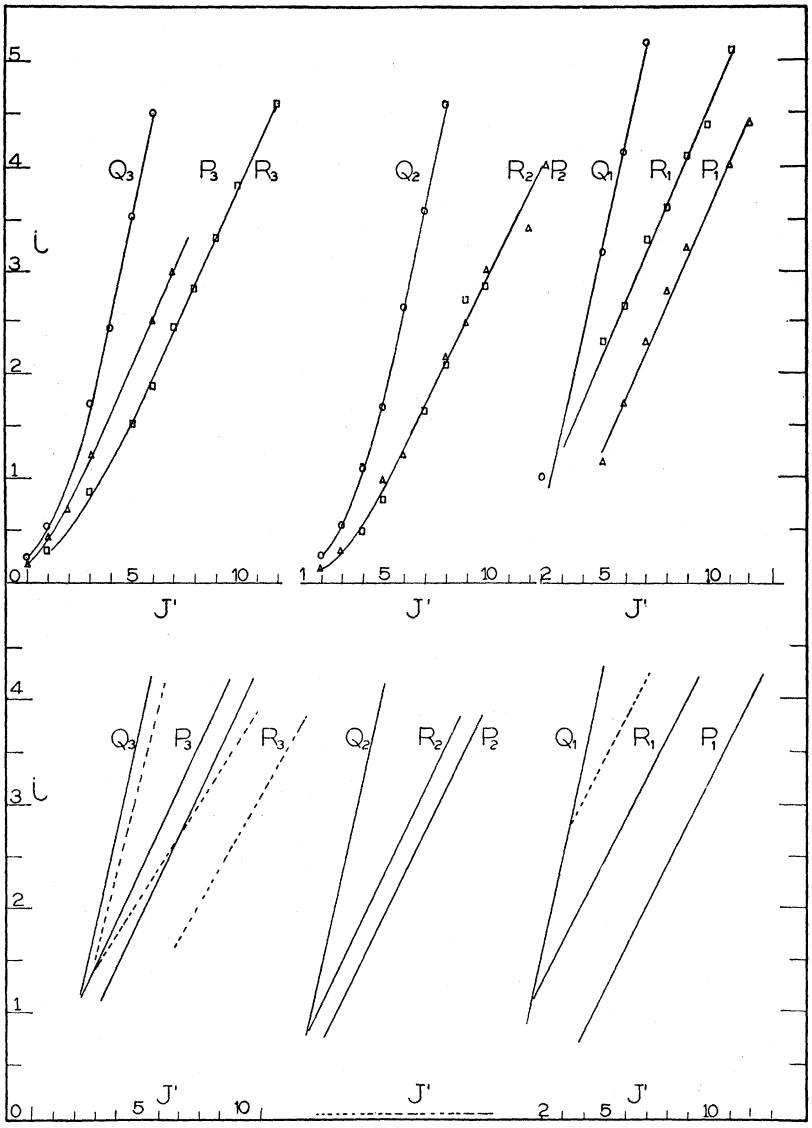

FIG. 2 (a). Comparison of the observed i factors with theoretical curves for case a (dotted lines) and case b (full lines).

theoretical curves for the Q_1 branch have arbitrarily been made equal. It will be seen that for the main branches, the experimental i factors increase linearly with J' for $J'>5$, and that the relative intensities of the branches agree closely with those from the case b formulas. An exception appears in the R_2 and P_2 branches, which are too nearly equal. The theoretical vanishing of the Q_2, R_2 and P_2 branches for pure case a is in agreement with the low observed intensities of these branches at the start.

The intensities of the satellite branches ($\Delta J \neq \Delta K$) shown in Fig. 2b are more sensitive to the type of coupling than are those of the main branches. In the lower part of the figure, the straight lines are the theoretical values for case a, and the hyperbolic curves of very low intensity are those for case b. The scale of the theoretical curves has been reduced throughout by a factor of 2 to render them comparable with the experimental values. Therefore it is apparent that the observed satellite branches are much

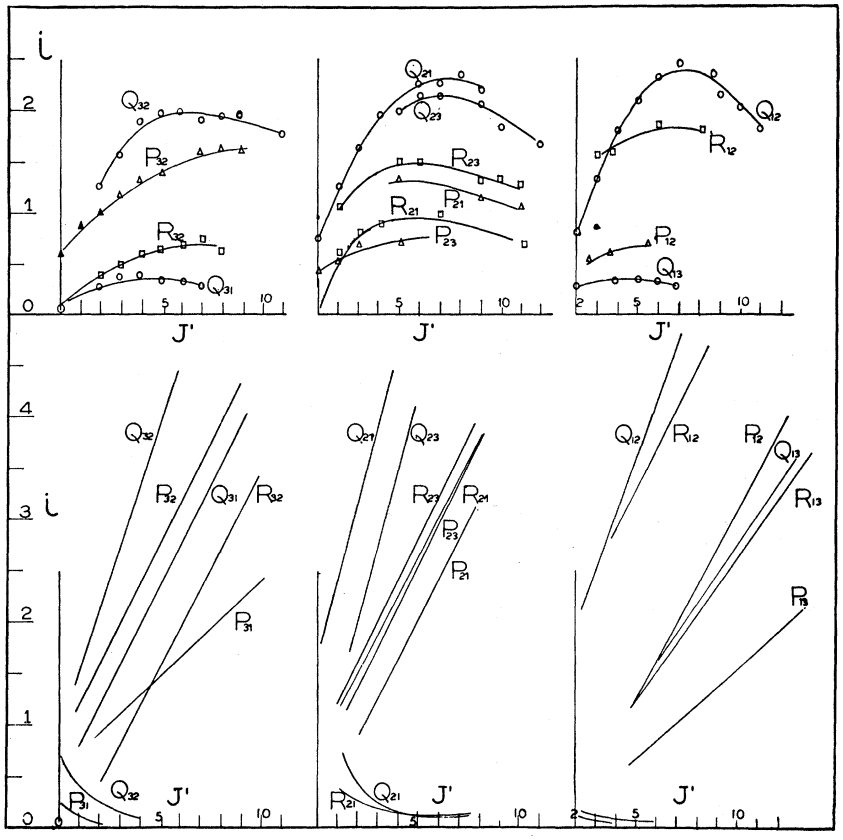

FIG. 2 (b). Intensities of satellite branches ($\Delta J \neq \Delta K$).

weaker than predicted for pure case a, becoming more so at higher values of J'. The relative order of intensity of the branches appears on the whole to be in fair agreement with theory, the outstanding discrepancies being an undue faintness of the Q_{31}, P_{23} and Q_{13} branches.

In conclusion, we have tested the validity of our experimental i factors by applying the sum rule for the final states. From Eq. (4), the sum of the i factors for all transitions to a given final state should be proportional to the weight of that level, $2J''+1$, so that

$$\sum_{J'} i/(2J''+1) = \text{const.}$$

This requirement was found to be accurately fulfilled, the average values of the constant obtained for the F_1, F_2 and F_3 levels being 1.02 ± 0.02, 1.01 ± 0.005 and 1.04 ± 0.02, respectively.